Phase transitions in a continuum model of the classical Heisenberg magnet: The antiferromagnetic system

Enrique Lomba
Instituto de Química Física Rocasolano, Consejo Superior de Investigaciones Científicas, Serrano 119, E-28006 Madrid, Spain

Jean-Jacques Weis
Laboratoire de Physique Théorique et Hautes Energies, Bâtiment 211, Université de Paris-Sud, 91405 Orsay Cedex, France

George Stell
Department of Chemistry, State University of New York at Stony Brook, Stony Brook, New York 11794-3400
(Received 28 March 1994; revised manuscript received 24 June 1994)

We model an antiferromagnetic fluid by a system of hard spheres with embedded classical Heisenberg spins with antiferromagnetic coupling constants. In this system we find from Monte Carlo simulation strong evidence of an order-disorder transition between paramagnetic and antiferromagnetic spatially disordered states, which also appears in an appropriate integral equation theory (reference hypernetted chain). We do not find direct simulation evidence of the presence of gas-liquid coexistence, but find such coexistence via the mean spherical approximation internal energy, which predicts a first-order gas-liquid transition. Analysis of the mean spherical results provides a tentative scenario concerning the way the line of Néel transitions approaches a liquid-gas coexistence curve.

PACS number(s): 61.20.Gy, 64.60.Cn

I. INTRODUCTION

This work is part of a continuing effort to extend our understanding of the phase transitions present in disordered magnetic materials. In a previous work [1] we have studied in some detail a fluid of hard spheres with embedded classical Heisenberg spins with ferromagnetic interactions. In the system considered, the interaction potential was taken to be

$$\beta u(12) = \begin{cases} \infty, & r < \sigma \\ \beta J(r)\Phi^{110}(12), & r \geq \sigma, \end{cases} \tag{1.1}$$

with

$$\beta J(r) = -J\frac{e^{-z(r-\sigma)}}{r}. \tag{1.2}$$

Here the rotational invariant $\Phi^{110}(12) = \mathbf{s}_1 \cdot \mathbf{s}_2$, where $\mathbf{s}_i$ is a unit vector describing the orientation of the spin of particle i, σ is the hard sphere diameter, $\beta = 1/k_BT$, where T is the temperature and k_B Boltzmann's constant, and r is the distance between two hard sphere centers. In Ref. [1], as well as in the present work, the value of z was $1/\sigma$. The behavior of the ferromagnetic system ($J > 0$) turned out to be fairly rich. Thus, we were able to determine, via Gibbs ensemble Monte Carlo simulation (GEMC) a gas-liquid coexistence curve, and to produce estimates of the loci of the Curie points (paramagnetic-ferromagnetic transition points), by means of integral equation theory together with canonical ensemble (NVT) Monte Carlo. For sufficiently low temperatures the order-disorder and gas-liquid transition were found to be coupled and, on the low density side of the coexistence region, the system to be organized into magnetized droplets. The line of Curie points appears to have a critical end-point at the gas-liquid spinodal. The purpose of the present paper is to examine the phase diagram in the case where antiparallel (antiferromagnetic) ordering of the spins is favored, i.e., the coupling constant J in Eq. (1.2) is negative. As for the ferromagnetic system, most of our results will be from integral-equation theory, specifically the mean spherical approximation (MSA) and reference hypernetted chain (RHNC) equation. On the basis of extensive earlier experience with these equations [1,2], we expect the MSA to be useless as a means of picking up any evidence of antiferromagnetic ordering. The MSA is intrinsically linear in its response to the coupling strength of the interaction between particles, but in the context of fluid-state integral-equation approach that cannot make use of sublattices to describe staggered order, a description of antiferromagnetic ordering requires nonlinear terms to ensure adequate coupling between the spherically symmetric and orientational dependent components of the correlation. On the other hand, the MSA can be expected to detect gas-liquid transitions via its internal energy, which provides a useful mean-field theory. In contrast, the nonlinear RHNC equation is capable of describing antiferromagnetic correlations, whereas the direct information it yields concerning gas-liquid transitions is known to be seriously unreliable, so we do not attempt to make use of this information in our analysis.

To monitor and supplement these theoretical predictions, and also to provide a qualitative picture of the orientational structure inside the ordered phase, not accessible to the integral equations, we have performed canonical ensemble Monte Carlo simulations.

The rest of the paper can be sketched as follows. In Sec. II we recall some of the main features of the MSA solution for the Heisenberg spin fluid, which are essential to the determination of the phase coexistence from MSA thermodynamics. In Sec. III we briefly discuss the RHNC results, including peculiarities of the well-known artificial singular behavior of this approximation in the presence of phase transitions (spinodal behavior and square root branch point singularities). Finally, in Sec. IV we present the Monte Carlo results and in Sec. V a discussion of the significance of our results. For full details of numerical procedures and techniques here applied we refer the reader to Ref. [1].

II. THERMODYNAMICS AND PHASE COEXISTENCE IN THE MEAN SPHERICAL APPROXIMATION

As mentioned in Ref. [1], the paramagnetic-antiferromagnetic transition is signalled by the divergence of the susceptibility

$$\chi_{220} = 1\Big/\left[1 - \frac{4\pi\rho}{5}\int_0^\infty r^2 c^{220}(r)dr\right], \tag{2.1}$$

where c^{220} is the (220) angular projection of the direct correlation function $c(12)$ in the spatial reference frame. Unfortunately, the MSA, due to its linear dependence on the potential (1.1), sets the projection c^{220} to zero so that it is not useful in connection with Eq. (2.1).

On the other hand, because the spin-spin interaction results in a net attraction between particles, irrespective of the sign of the coupling constant [1], the MSA might be able to predict a gas-liquid transition. This turns out, however, to be possible only if the thermodynamic route that starts with the internal energy is followed. Due to the MSA decoupling of the angle averaged pair correlation function g^{000} from the spin-spin interaction, it will not be possible to determine a gas-liquid spinodal from the divergence of the inverse compressibility. The thermodynamic properties of the system with interaction (1.1) in the MSA have been given by Høye and Stell [2]. Basically the problem reduces to finding the roots of the equation

$$u_0^3 + u_1^2 - \frac{1}{4}z^2 u_0 = 0, \tag{2.2}$$

with

$$u_0 = 6\xi K(1-\omega v/K)^2,$$

$$u_1 = -3\xi K(1-\omega v/K)(1-\gamma v/K),$$

where $\omega = (e^{-z}-1)/2z$, $\gamma = (e^{-z}+1)/2z$, $K = J/3$, and $\xi = \pi\rho\sigma^3/6$. Here v is related to the excess internal energy through

$$\beta U^{ex}/N = -\frac{3}{2}v(\xi, J), \tag{2.3}$$

which is a convenient starting point. From the knowledge of v, the excess free energy can be computed by a standard charging procedure [3], scaling J with a charging parameter λ and integrating

$$\beta(A - A^{HS})/N = -\frac{3}{2}\int_0^1 v(\xi, \lambda J)d\lambda. \tag{2.4}$$

It can be shown that, in contrast to the dipolar hard sphere case [3], the integration cannot be performed explicitly. The hard sphere contribution to the free energy can be estimated from the Carnahan-Starling equation of state, and thus one finally gets

$$\beta A/N = -\frac{3}{2}\int_0^1 v(\xi, \lambda J)d\lambda + \frac{2}{1-\xi} + \frac{1}{(1-\xi)^2}, \tag{2.5}$$

where a temperature-dependent constant has been omitted. The pressure and chemical potential must now be computed from the relations

$$\beta P = \rho^2\left(\frac{\partial \beta A/N}{\partial \rho}\right)_T \tag{2.6}$$

and

$$\beta\mu = \beta A/N + \rho\left(\frac{\partial \beta A/N}{\partial \rho}\right)_T. \tag{2.7}$$

These expressions yield fully consistent thermodynamics. The density dependence of P and μ exhibits a van der Waals loop characteristic of a mean field theory as it should be expected. The coexistence curve is obtained from the solution of the two nonlinear equations

$$\begin{aligned}\beta P(J, \rho_g) &= \beta P(J, \rho_l),\\ \beta\mu(J, \rho_g) &= \mu(J, \rho_l).\end{aligned} \tag{2.8}$$

Obviously the critical behavior obtained will be classical. It is worth remarking that the construction just described is only feasible in the antiferromagnetic system since in this case Eq. (2.2) gives real solutions for all physical values of ρ and J, whereas in the ferromagnetic case, the possible gas-liquid coexistence will be buried inside the boundary of complex solutions of Eq. (2.2).

III. SINGULARITIES AND CRITICAL BEHAVIOR IN THE RHNC EQUATION

The RHNC equation has been solved in the way described in Ref. [1] and details will be omitted here. We have tested the accuracy by comparing structural and thermodynamic properties in the dense paramagnetic region with exact MC results (for details of the latter see below). Figure 1 illustrates the comparison for the projection g^{000}, describing average spatial pair arrangement, and h^{220}, accounting for colinear orientational ordering of pairs of spins, irrespective of direction (parallel or an-

tiparallel), of the pair distribution functions at $\rho\sigma^3 = 0.8$ and $T^* = 3/|J| = 1.5$. (The factor 3 is introduced to be consistent with previous definitions [1] of the reduced T in terms of $K = J/3$.) The agreement is quite good, as is that for the thermodynamic properties. The values for the internal energy and compressibility factor are $\beta u^{\mathrm{RHNC}}/N = -4.195$ and $\beta P^{\mathrm{RHNC}}/\rho = 6.04$, respectively, compared to the MC values $\beta u^{\mathrm{MC}}/N = -4.20$, and $\beta P^{\mathrm{MC}}/\rho = 6.22$. However, the hypernetted chain approximation and variants such as the RHNC equation are already known to be unreliable in their predictions concerning gas-liquid criticality and coexistence. As already noted for the Heisenberg ferrofluid [1] and other systems [4], the RHNC equation has a no-solution region whose origin is different depending on density. At low density, the RHNC no-solution boundary is characterized by a square root branch point (SRBP). The inverse susceptibility χ_{220}^{-1} remains finite and near the SRBP can be fitted to

$$\chi_{220}^{-1} = a\sqrt{T^* - T_s^*} + b, \tag{3.1}$$

where T_s^* denotes the reduced temperature at which the numerical solution of the RHNC breaks down. This behavior is shown in Fig. 2 for $\rho\sigma^3 = 0.01$. Quite remarkably, and similar to the ferrofluid case [1] the isothermal compressibility χ_{000} exhibits the same singular behavior.

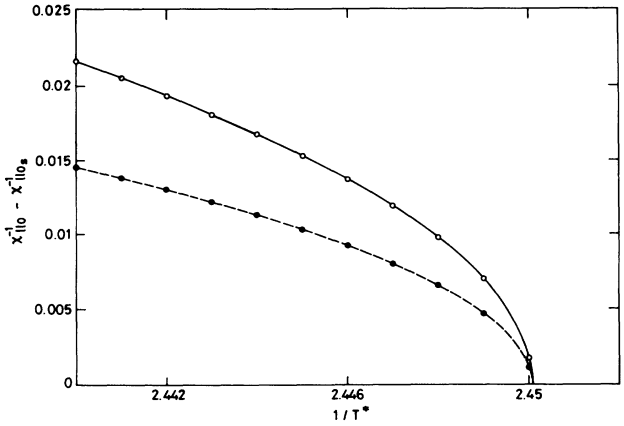

FIG. 2. Variation of the RHNC inverse isothermal compressibility and χ_{220}^{-1} in the vicinity of the nonsolution line at low density ($\rho\sigma^3 = 0.01$). Direct RHNC results are denoted by solid circles and lines correspond to a nonlinear fit to Eq. (3.1).

At high density the RHNC no-solution boundary is characterized by a divergence of the susceptibility χ_{220}, which follows a power law near the boundary,

$$\chi_{220}^{-1} = a(T^* - T_{s_1}^*)^{-\gamma} \tag{3.2}$$

at $\rho\sigma^3 = 0.9$ (cf. Fig. 3). The apparent value of γ ($\gamma = 0.99$) is very close to the classical value of unity, suggesting that unity is the true RHNC value. The isothermal compressibility remains finite. The magnitude of the exponent decreases with density and the divergence has a smooth crossover towards the SRBP behavior. The

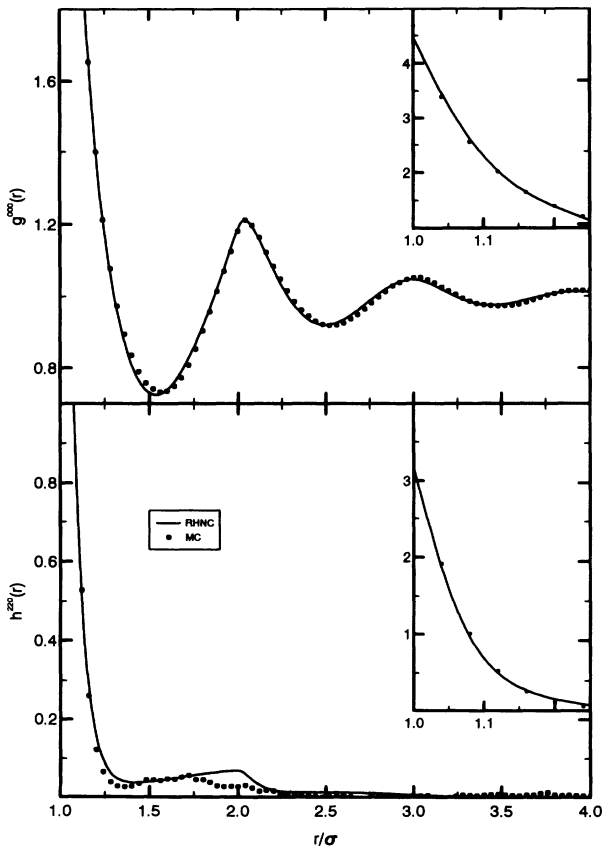

FIG. 1. g^{000} and h^{220} projections of the pair distribution function for the Heisenberg antiferromagnetic spin fluid in the paramagnetic phase ($\rho\sigma^3 = 0.8$, $T^* = 1.5$). RHNC results (lines) vs MC data (solid circles).

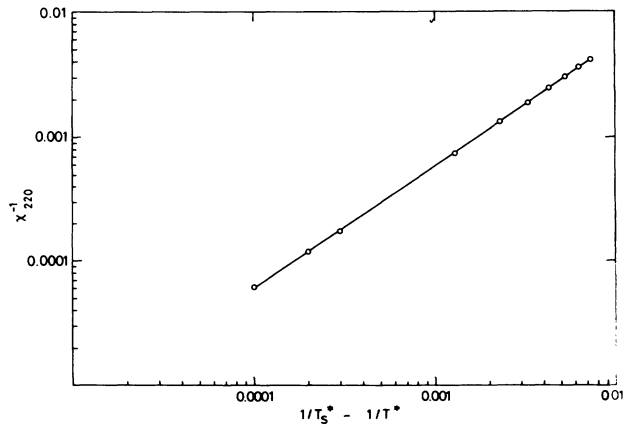

FIG. 3. RHNC χ_{220}^{-1} in the vicinity of the Néel temperature at high density ($\rho\sigma^3 = 0.9$). Direct RHNC results are denoted by solid circles and lines correspond to a nonlinear fit to Eq. (3.2).

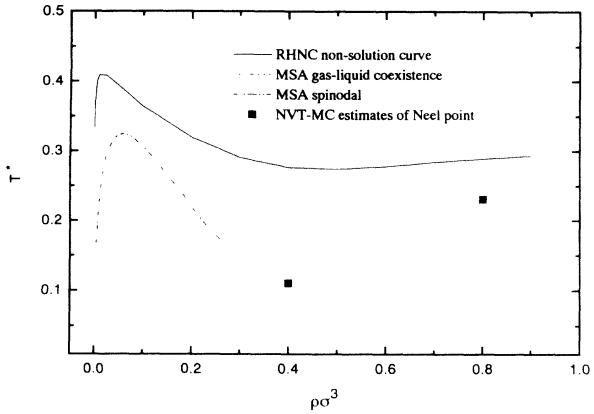

FIG. 4. No-solution line of the RHNC equation of the Heisenberg antiferromagnetic spin fluid and MSA estimate of the gas-liquid coexistence curve and spinodal. MC estimates of Néel points are represented by solid squares.

crossover density is hard to determine with precision but should be close to $\rho\sigma^3 \sim 0.2$. In Fig. 4 we have plotted the nonsolution line of the RHNC equation together with the MSA gas-liquid coexistence curve and MC estimates of the order-disorder transition (see below). An intriguing feature in this figure is the proximity of the MSA gas-liquid critical point and the maximum in the no-solution curve of the RHNC equation. Whether the SRBP singularity of the RHNC equation should be regarded here as a RHNC caricature of a gas-liquid transition, as it is in the case of other model potentials [4], is an unresolved question.

IV. MONTE CARLO STUDIES OF THE ANTIFERROMAGNETIC TRANSITION

Here we shall discuss the use of computer simulation to help determine the location of order-disorder transitions. The paramagnetic-antiferromagnetic transition temperature (the Néel-point temperature) can be obtained from the point where the order-parameter vanishes. However, similar to what is observed in the simulations of the Heisenberg ferromagnet [1,5] with a finite number of particles, the variation of the order parameter with temperature shows appreciable "rounding" near the phase transition, rendering a precise determination of the transition temperature impossible. In simulations of lattice spin systems these shortcomings have been circumvented by taking advantage of finite size scaling analysis together with efficient spin sampling methods, histogram techniques, etc. [6]. Although these methods translate readily to the continuum case and have, in fact, been applied successfully to locate Curie temperatures in the ferromagnetic Heisenberg system [7], they are nevertheless, too demanding in computer time to justify their application to the present exploratory study. For this reason we limited ourselves to perform Monte Carlo calculations in the canonical ensemble for a system of $N = 500$ spins in a cubic box with periodic boundary conditions, the preceding discussion implying that the results should be viewed only as providing a qualitative description of the phases.

The MC results for the thermodynamic properties and order parameters are summarized in Table I. The ordering of the system was monitored through the parameter S_2 which is the ensemble average of the largest eigenvalue of the ordering matrix $\mathbf{Q}$ whose elements are given by [8]

$$Q_{\alpha\beta} = \frac{1}{N}\sum_{i}^{N}\left(\frac{3}{2}u_\alpha^i u_\beta^i - \frac{1}{2}\delta_{\alpha\beta}\right), \tag{4.1}$$

where u_α^i ($\alpha = x, y, z$) is the Cartesian component of the unit vector describing the orientation of the spin embedded in particle i. The variation of the order parameter S_2 can be followed in Table I. At the two highest densities, S_2 takes appreciable values (≈ 0.5) for $T^* \sim 0.15$ ($\rho\sigma^3 = 0.4$) and $T^* \approx 0.22$ ($\rho\sigma^3 = 0.8$) and these values of T^* can be taken as rough estimates of the temperatures at which ordering sets in in the finite system. The snapshot of a configuration of spins at $T^* = 0.1875$, $\rho\sigma^3 = 0.8$ (Fig. 5) clearly shows that for this thermodynamic state the preferential ordering of the spins around a given particle has antiferromagnetic character.

The change in fluid structure when crossing the transition temperature is further illustrated in Figs. 6–8 showing the projection g^{000}, h^{110}, and h^{220} (defined in Ref. [1]) of the molecular pair distribution function $g(12)$

TABLE I. Thermodynamics and order parameter S_2 of the Heisenberg antiferromagnetic spin fluid from NVT Monte Carlo simulation. N_{cf} is the number of configurations and N the number of particles.

$\rho\sigma^3$	J	T^*	N_{cf}/N	$\beta u/N$	$\beta P/\rho$	S_2
0.01	-10.0	0.30	36000	-3.34	0.49	0.05
0.1	-8.6	0.349	60000	-3.86	0.34	0.05
	-10.0	0.30	50000	-5.02	0.21	0.05
	-20.0	0.15	40000	-15.47	-0.29	0.20
	-40.0	0.075	50000	-33.1	-0.84	0.23
	-60.0	0.05	30000	-53.8	-1.36	0.28
0.2	-10.0	0.30	52000	-5.63	0.22	0.06
	-12.0	0.25	80000	-7.43	0.03	0.07
	-15.0	0.20	100000	-7.43	-0.08	0.10
	-20.0	0.15	80000	-16.32	-0.26	0.40
	-25.0	0.12	110000	-21.9	-0.78	0.60
	-30.0	0.1	80000	-26.4	-1.16	0.44
0.4	-12.0	0.25	100000	-8.30	0.33	0.07
	-15.0	0.20	92000	-11.20	-0.09	0.11
	-20.0	0.15	40000	-17.04	-0.50	0.53
0.8	-10.0	0.30	50000	-8.06	5.06	0.07
	-12.0	0.25	80000	-10.12	4.51	0.11
	-12.06	0.238	70000	-10.80	4.32	0.20
	-13.0	0.231	52000	-11.53	4.11	0.40
	-14.0	0.214	48000	-13.08	3.63	0.59
	-16.0	0.1875	50000	-15.80	2.58	0.73
	-20.0	0.15	16000	-20.34	1.92	0.79

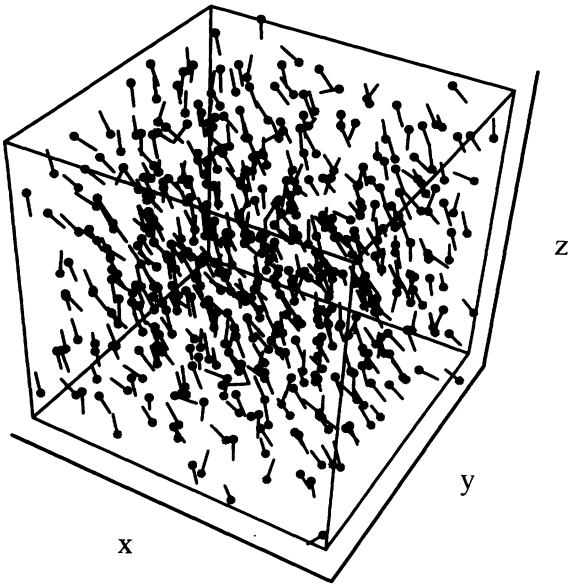

FIG. 5. Three-dimensional snapshot of an antiferromagnetic state at $\rho\sigma^3 = 0.8$, $T^* = 0.1875$. The spins are represented by lines with a dot indicating the direction of the spin. The hard sphere center is at the middle of the line. The side of the simulation box is 8.55σ long.

$[h(12) = g(12) - 1]$ at $\rho\sigma^3 = 0.8$. It is visible in the h^{220} projection which decays to zero for $T^* \geq 0.25$, whereas it shows long range orientational order for $T^* < 0.25$, in accord with the asymptotic relationship

$$h^{220}(r) \approx 5S_2^2 \quad (r \longrightarrow \infty). \tag{4.2}$$

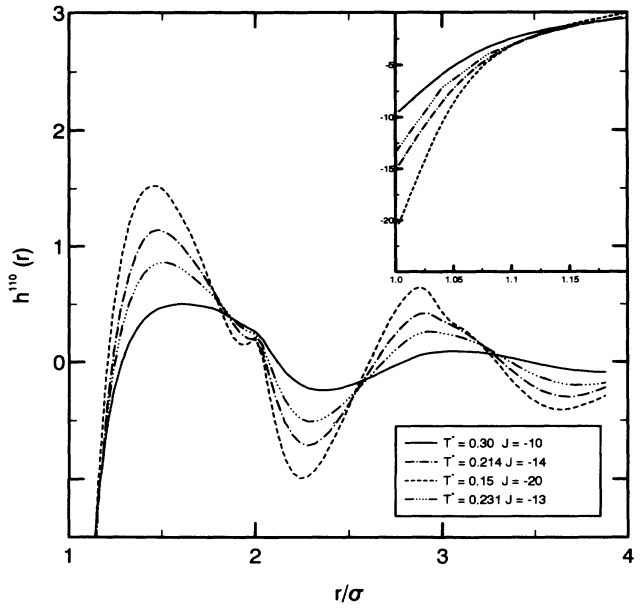

FIG. 6. The variation of the projection $h^{220}(r)$ of the pair distribution function with temperature at $\rho\sigma^3 = 0.8$.

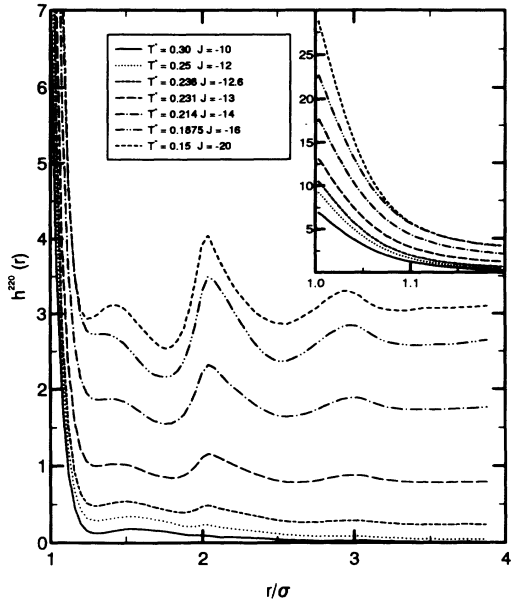

FIG. 7. The variation of the projection $h^{110}(r)$ of the pair distribution function with temperature at $\rho\sigma^3 = 0.8$.

As expected from the antiparallel ordering of neighboring spins, h^{110} is negative at contact and at large distances presents well defined oscillations around zero.

Upon increase of the coupling constant J (decrease of the temperature) the average pair distribution function, g^{000} is seen to develop a small peak at $r \sim 1.4\sigma$ indicating local formations of closely packed structures.

Snapshots of configurations in the low density region $\rho\sigma^3 = 0.1 - 0.3$ are shown in Figs. 9 and 10. Whereas above $T^* \approx 0.22$ system structure appears to be fairly

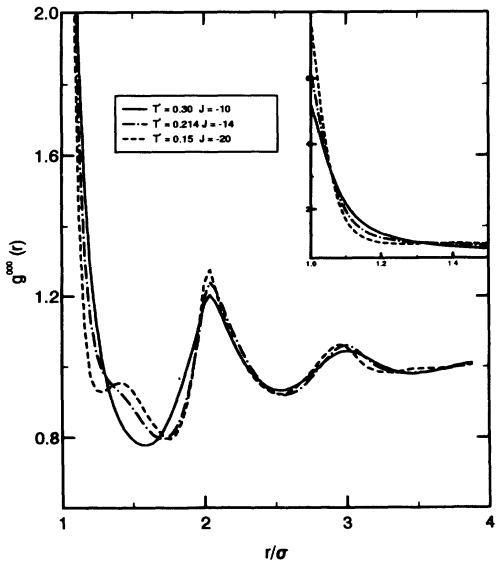

FIG. 8. The variation of the projection $g^{000}(r)$ of the pair distribution function with temperature at $\rho\sigma^3 = 0.8$.

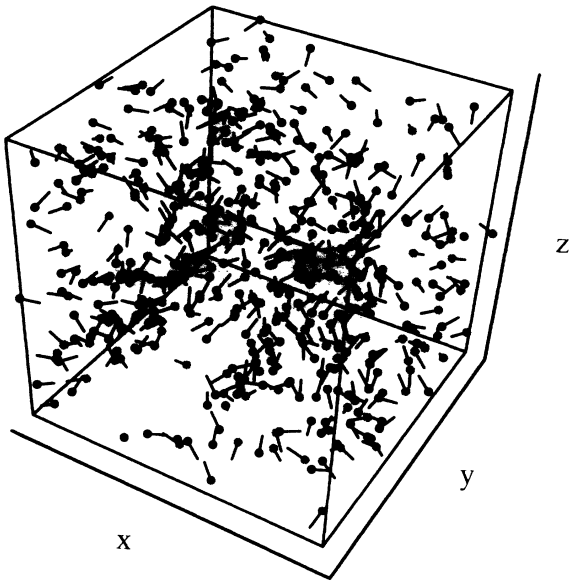

FIG. 9. Three-dimensional snapshot of a spin configuration at $\rho\sigma^3 = 0.2$ and $T^* = 0.25$. The box length is 13.57σ.

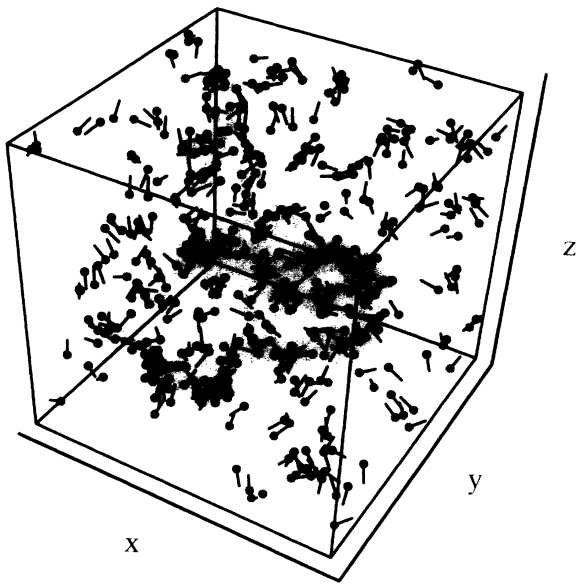

FIG. 11. Three-dimensional snapshot of a spin configuration at $\rho\sigma^3 = 0.01$ and $T^* = 0.30$. The box length is 36.84σ.

homogeneous (Fig. 9) with an order parameter $S_2 \sim 0$, more complex structural arrangements seem to occur at lower temperature (Fig. 10). These appear to be characterized by fairly connected regions in which the spins tend to align with antiferromagnetic order. As the average direction of alignment of the spins may vary from region to region, the global value of the order parameter turns out to be small (cf. Table I). This structure differs considerably from that of the ferromagnetic system, for which at comparable densities, strongly magnetized droplets typical of gas-liquid coexistence were observed. Whether the structural patterns found in the present case indicate coexistence between a gas and an antiferromagnetic liquid is less clear and cannot be decided without further free energy calculations. A few additional remarks can be made. Simulations using the GEMC method do not give evidence of a gas-liquid transition in the temperature range $T^* = 0.45 - 0.19$ in agreement with NVT calculations [9]. As we shall see in Sec. V, there is some independent complementary evidence that the gas-liquid critical point is to be expected below $T^* = 0.2$ or so. From Table I it is readily seen that states in the density range $0.1 < \rho\sigma^3 < 0.4$ with temperature $T^* \leq 0.20$ have negative pressure according to our canonical ensemble MC results. States in this range may be artificially stabilized by the periodic boundary conditions in a way that is masking the appearance of a critical point somewhere in this region. A marked difference with the ferromagnetic fluid is that in the latter instance successive layers of spins cooperate to lower the energy of the system, whereas in the antiferromagnetic system, due to alternating directions of the spins in adjacent layers some cancellation of the stabilization energies occurs.

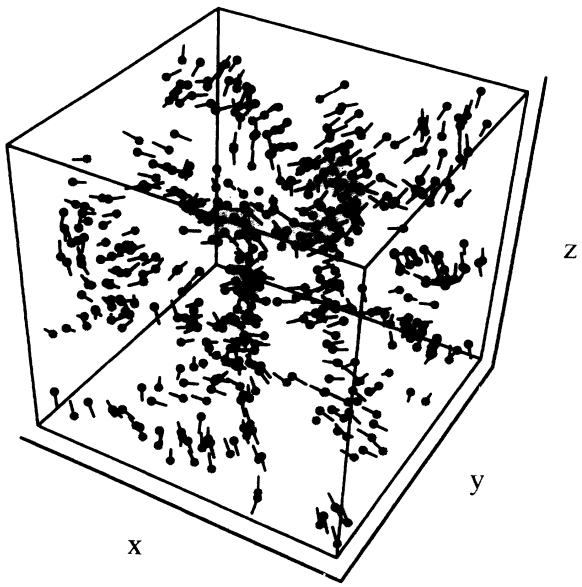

FIG. 10. Three-dimensional snapshot of a spin configuration at $\rho\sigma^3 = 0.1$ and $T^* = 0.075$. The box length is 17.10σ.

Finally at even lower density $\rho\sigma^3 = 0.01$ ($T^* = 0.30$) the particles show a strong tendency to associate into pairs with antiparallel ordering of the spins. This behavior is manifest in the snapshot presented in Fig. 11 and also in the large negative value of the projection h^{110} near contact. However, there is no long-range antiparallel ordering.

V. DISCUSSION OF THE RESULTS

Perhaps the most striking and significant of our results is the strong Monte Carlo evidence we find for a

paramagnetic-antiferromagnetic transition in the liquid state. These preliminary results are consistent with the appearance of a line of Néel points in the liquid region of the $\rho^* - T^*$ plane that spans the two points indicated in Fig. 4, and perhaps meets a gas-liquid coexistence curve in the near vicinity of the lower of those points. In a lattice-gas version of the model treated here on a cubic lattice consisting of two interlaced sublattices, the lattice symmetry would provide a natural length associated with staggered order. As a result one would expect as a matter of course the appearance of a λ line of Néel points. In the fluid version considered here, it has been less obvious what to expect in the absence of such lattice symmetry. It is for this reason that the Monte Carlo evidence for the antiferromagnetic state is particularly interesting.

Although we are unable to discern from our MC calculations any direct evidence pertaining to the location of a gas-liquid transition, the MSA estimate of where this transition is located, together with our MC estimate of the location of the λ line of Néel points, provides us with a tentative picture of the way the gas-liquid and Néel transitions are situated with respect to each other.

In order to use the MSA results to estimate where the true gas-liquid transition lies, we shall argue that the trends one observes in comparing the MSA and the true gas-liquid coexistence curve in the restricted primitive model (RPM) can also be expected in the case of the antiferromagnetic Heisenberg fluid, but they will probably be less pronounced.

In the RPM, comparisons of the MSA coexistence curve with the recent simulation results of Caillol [10] and of Orkoulas and Panagiotopoulos [11] show that the true gas-liquid critical point is at a considerably lower temperature and a somewhat higher density than the MSA critical point, and that the true coexistence curve under the critical point would be somewhat more sharply peaked than the MSA curve shown on a ρ^*-T^* plot such as that of Fig. 4.

The reason we can expect these same trends in the case of the antiferromagnetic Heisenberg fluid lies in the fact that the RPM is an antiferromagnetic Ising fluid with a Coulombic $J(r)$. In an antiferromagnetic fluid (Heisenberg or Ising) one expects the thermodynamic effect of the higher-order terms in J missing in the MSA to counteract, and thus weaken the effect of the lowest-order-J^2 terms. In particular, this will lower the gas-liquid critical temperature and change somewhat the shape of the coexistence curve. However, this effect will tend to be more pronounced in the Ising case than in the Heisenberg case—for example, the term of order J^3 is three times larger relative to the J^2 term in the Ising case than in the Heisenberg case. Similarly, when one goes from a $J(r)$ of Yukawa form to one of Coulomb form, the relative counteracting effect of the higher-order terms can again be expected to be enhanced. Since the RPM does show a gas-liquid critical point, it seems reasonable to also expect such a point in the antiferromagnetic Heisenberg fluid, but at lower temperature than that given by the MSA, with an altered coexistence-curve shape. On the basis of this line of reasoning one might expect a critical point that is likely to be near $T^* = 0.2$ in temperature, as well as somewhat higher in density than the MSA critical point [12]. This would give rise to the λ line of Néel points meeting the coexistence curve at a density substantially higher than the critical density. Our discussion of the gas-liquid transition must remain tentative, however, until there is confirmation of the gas-liquid transition from simulation results.

ACKNOWLEDGMENTS

The authors would like to thank F. Bresme who performed several MSA calculations presented here and N.G. Almarza who kindly shared with us details of his GEMC calculations. D. Levesque is also acknowledged for numerous helpful discussions. Part of this work has been financed by Spanish Dirección General de Investigación Científica y Técnica (DGICYT) under Grant No. PB91-0110. G.S. gratefully acknowledges the National Science Foundation for their support of his contribution to this work.

[1] E. Lomba, J.J. Weis, N.G. Almarza, F. Bresme, and G. Stell, Phys. Rev. E **49**, 5169 (1994).

[2] J.S. Høye and G. Stell, Phys. Rev. Lett. **36**, 1569 (1976). See, also, R.M. Stratt, *ibid.* **53**, 1305 (1984); S.G. Desjardins and R.M. Stratt, J. Chem. Phys. **81**, 6232 (1984), for extensions of this work; and P.C. Hemmer and D. Imbro, Phys. Rev. A **16**, 380 (1977) for a mean-field treatment of a spin fluid.

[3] G.S. Rushbrooke, G. Stell, and J.S. Høye, Mol. Phys. **26**, 1119 (1973).

[4] L. Belloni, J. Chem. Phys. **98**, 8080 (1993). See also E. Lomba, J.S. Høye, and G. Stell, Mol. Phys. **79**, 523 (1993).

[5] K. Binder, in *Phase Transitions and Critical Phenomena*, edited by C. Domb and M.S. Green (Academic, New York, 1976), Vol. 5b.

[6] See, e.g., K. Chen, A.M. Ferrenberg, and D.P. Landau, Phys. Rev. B **48**, 3241 (1993); C. Holm and W. Janke, *ibid.* **48**, 936 (1993), and references therein.

[7] M. Nijmeyer, J.J. Weis, and D. Levesque (unpublished).

[8] R. Eppenga and D. Frenkel, Mol. Phys. **52**, 1304 (1984).

[9] N.G. Almarza (private communication).

[10] J.M. Caillol, J. Chem. Phys. **100**, 2161 (1994).

[11] G. Orkoulas and A.Z. Panagiotopoulos, J. Chem. Phys. **101**, 1452 (1994).

[12] The RPM critical point occurs at $\rho^* = 0.014$, $T^* = 0.079$ according to the MSA, while a recent simulation study [11] yields the estimate $\rho^* = 0.025$, $T^* = 0.053$, which we regard as a reasonable guide to the true RPM values.